

VIBRATION OF A ROTATING BEAM WITH TIP MASS†

S. V. HOA

*Department of Mechanical Engineering,
Concordia University, Montreal, Canada H3G 1M8*

(Received 30 September 1978, and in revised form 11 July 1979)

The vibration frequency of a rotating beam with tip mass is investigated. The finite element method is used, a third order polynomial being assumed for the variation of the lateral displacement. The effects of the root radius, the setting angle and the tip mass are incorporated into the finite element model. The results are compared with results from previous authors utilizing Myklestad and extended Galerkin methods. The results show that the setting angle has a significant effect on the first mode frequencies but not on the high frequencies. The tip mass tends to depress the frequencies at low speeds of rotation but it tends to increase the frequencies at high speeds of rotation. The results of this work have applications in wind turbine rotors, helicopter rotors, etc., and the method used here can be extended to investigate the vibration frequency of flexible blade auto cooling fans.

1. INTRODUCTION

In many structural designs, tip masses are utilized. The function of the tip mass can be to increase the airflow as in the case of a dynamic inducer for a wind turbine; it can be to modify the vibration frequency of components as in the case of a helicopter rotor or it can be to increase the flexing motion of the blade in flexible blade auto cooling fans [1]. It was with the intention to obtain the vibration frequency of a rotating blade with a weighted edge in the case of a flexible blade auto cooling fan that this work was initiated.

The problem of determining the influence of a tip mass on the natural frequencies of transverse vibration of a uniform rotating beam clamped at one end was first studied in connection with the design of helicopter blades. Handelman, Boyce and Cohen [2] derived the appropriate partial differential equations describing the motion of a rotating beam with a tip mass and obtained upper and lower bounds for the first mode frequency. Subsequently, Boyce and Handelman [3] derived the corresponding equations for beams of variable density and flexural rigidity and obtained results for a uniform beam using a variety of perturbation methods. Jones [4] used an integral equation method to obtain improvable lower bounds for the second mode frequencies.

The equations of motion derived in the above works are complex and the method of solution used cannot be easily extended to problems of further complication such as the vibration frequency of a rotating blade with a tip mass, which represents a flexible blade fan much more closely. The numerical solutions to this problem include the work of Kumar [5], in which the author used the Myklestad method to obtain both out of plane and in plane vibration frequencies. The finite element method was used by Putter and Manor [6].

† Presented at the Fourth Symposium on Engineering Applications of Solid Mechanics, Ontario Research Foundation, 25–26 September 1978.

The above-mentioned works produced significant contributions to the understanding of the vibration frequencies of rotating beams with tip masses. However, in most of these works only vibration out of the plane of rotation was considered (where the setting angle θ is equal to zero). The work of Kumar [5] includes also consideration of the case of in-plane vibration where the setting angle θ is equal to 90° . The purpose of this paper is to develop a finite element model for obtaining the vibration frequencies of a rotating beam with a tip mass, with consideration taken of the effect of the setting angle θ . In their study on the vibration frequencies of rotating cantilevered plates, Dokainish and Rawtani [7] incorporated the setting angle into their analysis. The effect of this angle was also included and discussed for a beam without a tip mass by Wang *et al.* [8].

2. THEORY

The cantilever beam is considered mounted on the periphery of a rotating disc of radius r in such a manner that the mid-plane of the beam is inclined to the plane of rotation of the disc at an angle θ , called the setting angle, as shown in Figure 1. X, Y, Z is a system of

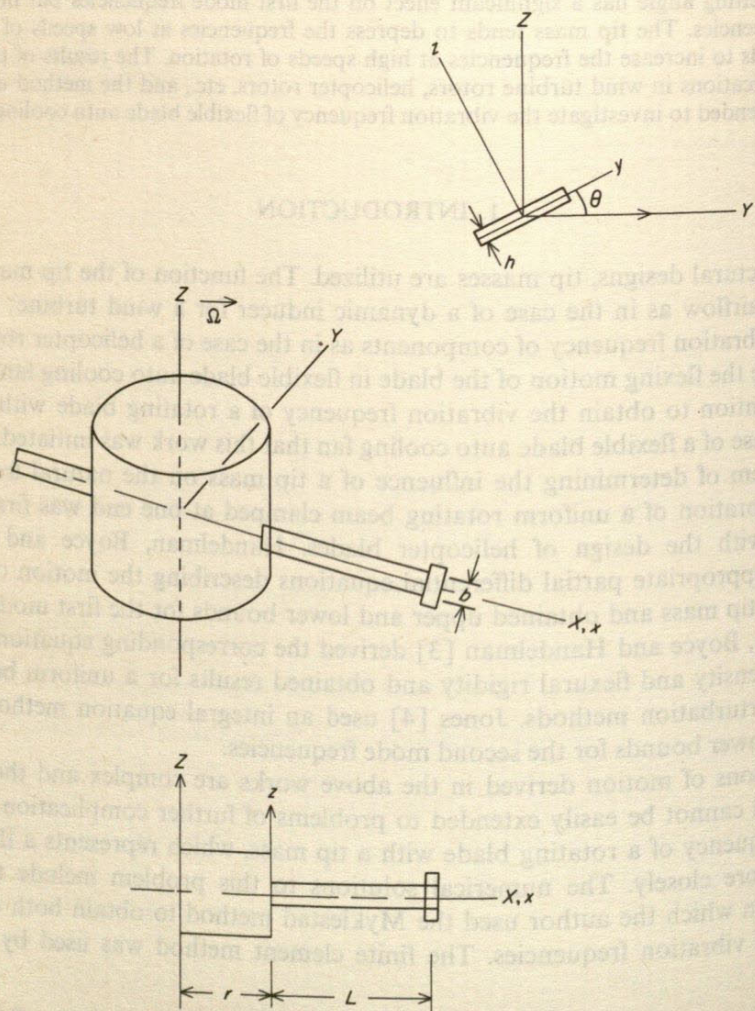


Figure 1. Geometry, see reference [8].

Cartesian global co-ordinate axes with the origin at the center of the rotating disc while x, y, z is a system of Cartesian global co-ordinate axes with the origin at the root of the beam and with orientations along the major dimensions of the beam: i.e., the x axis is along the length of the beam, the y axis along the width and the z axis along the thickness of the beam (a list of nomenclature is given in the Appendix). The disc is assumed to be rigid.

2.1. FORCES ACTING ON THE BEAM

The analysis of a rotating beam without a tip mass is considered here. The effect of a tip mass is included later. For a beam undergoing lateral vibration, if w is the deflection in the z direction of an arbitrary point on the middle plane (xy plane) of the beam, its instantaneous location in the x, y, z system of co-ordinates can be taken as (x, w) .

The radial component of the centrifugal force per unit volume acting on an element of the beam at x is given by

$$F_r = \rho \Omega^2 (r + x), \quad (1)$$

where ρ is the mass per unit volume of the beam. As can be seen from Figure 2, a displacement of w along the z direction would result in a component $-w \sin \theta$ in the Y direction and a component $w \cos \theta$ in the Z direction. The force F_r can be resolved into two components along the Y and X directions:

$$F_x = F_r \simeq \rho \Omega^2 (r + x), \quad F_y = (r + x) \rho \Omega^2 [-w \sin \theta / (r + x)] = -\rho \Omega^2 w \sin \theta. \quad (2, 3)$$

The force F_y can be resolved into components along the y and z directions: i.e.,

$$F_y = F_Y \cos \theta = -\rho \Omega^2 w \sin \theta \cos \theta, \quad F_z = -F_Y \sin \theta = \rho \Omega^2 w \sin^2 \theta. \quad (4, 5)$$

The inertia force per unit volume of the beam is

$$F_{in} = \rho \ddot{w}, \quad (6)$$

where \ddot{w} denotes the second derivative of the displacement w with respect to time.

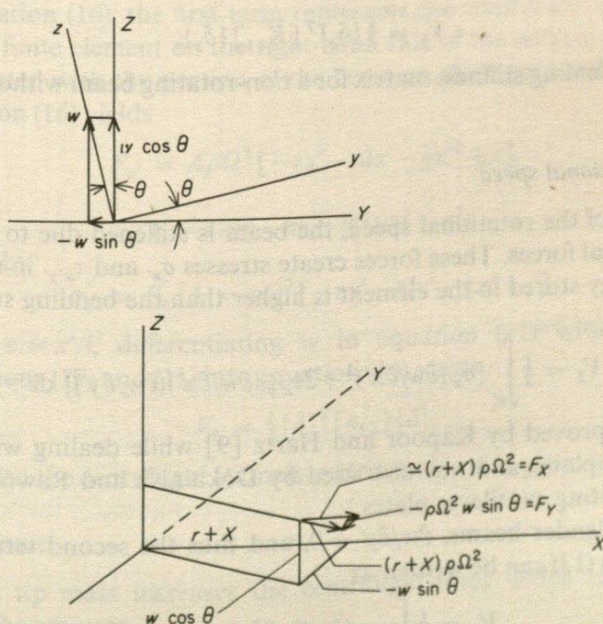


Figure 2. Displacement and force components.

According to D'Alembert's principle, the total force acting on the beam in the z direction is given by

$$F = F_z - F_{in} = \rho\Omega^2 w \sin^2 \theta - \rho\ddot{w}. \quad (7)$$

2.2. STIFFNESS MATRICES

2.2.1. Non-rotating beam without tip mass

For a non-rotating beam without a tip mass undergoing transverse vibration, the potential energy is given by the expression

$$V = (EI/2) \int_L (\partial^2 w / \partial x^2)^2 dx, \quad (8)$$

where x represents the co-ordinate for the beam. In the finite element formulation, the beam is divided into elements and the above expression is also applicable; i.e.,

$$V_1 = (EI/2) \int_l (\partial^2 w / \partial x'^2)^2 dx', \quad (9)$$

where x' represents the local co-ordinates for the element.

Let the displacement w be approximated by a third order polynomial:

$$w = c_1 + c_2 x' + c_3 x'^2 + c_4 x'^3. \quad (10)$$

Let $x' = le$, where l is the length of the element and ε is a non-dimensional variable. With c_1-c_4 expressed in terms of the nodal variables at the two ends a, b of the element, equation (10) can be written as

$$w = [D]\{\delta_b\}, \quad (11)$$

where

$$\begin{aligned} [D] &= [(1 - 3\varepsilon^2 + 2\varepsilon^3); (\varepsilon - 2\varepsilon^2 + \varepsilon^3); (3\varepsilon^2 - 2\varepsilon^3); (-\varepsilon^2 + \varepsilon^3)], \\ \{\delta_b\} &= \{w_a \ l w_{x'a} \ w_b \ l w_{x'b}\}^T. \end{aligned} \quad (11a)$$

Substituting equation (11) into equation (9) yields

$$V_1 = \frac{1}{2} \{\delta_b\}^T [K_{b1}] \{\delta_b\}, \quad (12)$$

where $[K_{b1}]$ is the bending stiffness matrix for a non-rotating beam without a tip mass and is given in Table 1.

2.2.2. Effect of rotational speed

Under the effect of the rotational speed, the beam is stiffened due to additional stresses created by centrifugal forces. These forces create stresses $\sigma_{x'}$ and $\tau_{x'y'}$ in the neutral surface, and the strain energy stored in the element is higher than the bending strain energy by the amount

$$V_2 = \frac{1}{2} \int_{v'} \{\sigma_{x'}(\partial w / \partial x')^2 + 2\tau_{x'y'}(\partial w / \partial x')(\partial w / \partial y')\} dv'. \quad (13)$$

Equation (13) was proved by Kapoor and Hartz [9] while dealing with the problem of stability analysis of plates and was also used by Dokainish and Rawtani [7] in studying the vibration of rotating cantilever plates.

For the case of slender beams, $\partial w / \partial y' = 0$, and thus the second term in equation (13) drops out. Equation (13) can be written as

$$V_2 = \frac{1}{2} \int_{v'} \sigma_{x'}(\partial w / \partial x')^2 dx' dy' dz'. \quad (14)$$

The stress $\sigma_{x'}$ can be obtained from the forces $F_{x'}$ and F_y in the plane $x'y'$. These forces are the local counterparts of F_x and F_y given in equations (2) and (4).

Since F_y creates bending stresses which are proportional to y' , the effects of these stresses cancel themselves out in the integration. The stresses due to axial forces $F_{x'}$ can be obtained as follows.

Consider the finite element shown in Figure 3. The centrifugal force associated with an infinitesimal length dx' of the element located at x' is

$$dF_{x'} = A\rho\Omega^2(r+nl+x')dx'. \quad (15)$$

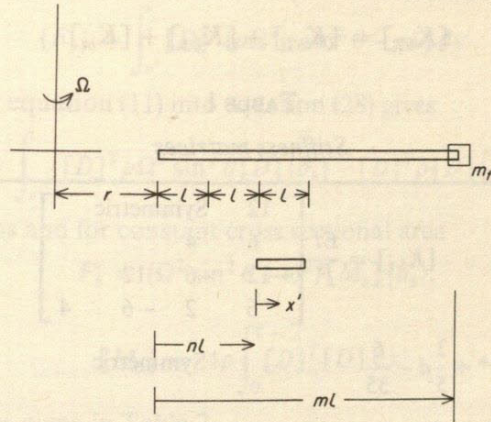


Figure 3. Location of finite element.

The force acting on any section at a distance x' from the left end of the element is

$$F_{x'} = A \int_{x'}^l \rho\Omega^2(r+nl+x')dx' + A \int_{(n+1)l}^{ml} \rho\Omega^2(r+x)dx, \quad (16)$$

where n is the number of elements before and not including the element under consideration. In equation (16), the first term represents the centrifugal force associated with the portion of the finite element on the right-hand side of the section and the second term is the force associated with the portion of the beam on the right hand side of the element. Integrating equation (16) yields

$$F_{x'} = A\rho\Omega^2[-rx' - nlx' - \frac{1}{2}x'^2 + c], \quad (17)$$

where

$$c = rl(m-n) + \frac{1}{2}l^2(m^2 - n^2). \quad (18)$$

The stress is given by

$$\sigma_{x'} = F_{x'}/A = \rho\Omega^2[-rx' - nlx' - \frac{1}{2}x'^2 + c]. \quad (19)$$

Replacing x' by $\varepsilon = x'/l$, differentiating w in equation (11) with respect to ε and substituting equations (19) and (11) into equation (14) yields

$$V_2 = \frac{1}{2}\{\delta\}^T [k_{b2}] \{\delta\}, \quad (20)$$

where $[K_{b2}]$ is called the centrifugal stiffness matrix and is also given in Table 1.

2.2.3. Effect of tip mass

Addition of the tip mass increases the centrifugal force which in turn increases the axial stress $\sigma_{x'}$ by the amount

$$\sigma_{x' \text{ tip}} = (r+L)m_t\Omega^2/A. \quad (21)$$

The additional potential energy is therefore

$$V_{\text{tip}} = \frac{1}{2} \int_{v'} \{(r+L)m_t \Omega^2/A\} (\partial w/\partial x')^2 dv', \quad (22)$$

which in matrix form is

$$V_{\text{tip}} = \frac{1}{2} \{\delta_b\}^T [K_{bt}] \{\delta_b\}, \quad (23)$$

where $[K_{bt}]$ is the tip mass stiffness matrix and is also given in Table 1.

The stiffness matrices for the elements of the rotating beam with tip mass $[K_{bt}]$ will be the sum of the matrices above: i.e.,

$$[K_{bT}] = [K_{b1}] + [K_{b2}] + [K_{bt}]. \quad (24)$$

TABLE 1
Stiffness matrices

$[K_{b1}] = \frac{EI}{l^3} \begin{bmatrix} 12 & & & \\ 6 & 4 & & \\ -12 & -6 & 12 & \\ 6 & 2 & -6 & 4 \end{bmatrix}$
$[K_{b2}] = Al\rho\Omega^2 \begin{bmatrix} \frac{6}{5}c^* + \frac{3}{5}d - \frac{6}{35} & & & \text{Symmetric} \\ \frac{c^*}{10} + \frac{d}{10} - \frac{1}{28} & \frac{2}{15}c^* + \frac{d}{30} - \frac{1}{105} & & \\ -\frac{6}{5}c^* - \frac{3}{5}d + \frac{6}{35} & -\frac{c^*}{10} - \frac{d}{10} + \frac{1}{28} & \frac{6}{5}c^* + \frac{3}{5}d - \frac{6}{35} & \\ \frac{c^*}{10} + \frac{1}{70} & -\frac{c^*}{30} - \frac{1}{60}d + \frac{1}{140} & -\frac{c^*}{10} - \frac{1}{70} & \frac{2}{15}c^* + \frac{d}{10} - \frac{3}{70} \end{bmatrix}$
$c^* = R'(m-n) + \frac{1}{2}(m^2 - n^2), \quad d = R' + n, \quad R' = r/l$
$[K_{bt}] = \frac{(r+L)m_t \Omega^2}{l} \begin{bmatrix} \frac{6}{5} & & & \text{Symmetric} \\ \frac{1}{10} & \frac{2}{15} & & \\ -\frac{6}{5} & -\frac{1}{10} & \frac{6}{5} & \\ \frac{1}{10} & -\frac{1}{30} & -\frac{1}{10} & \frac{2}{15} \end{bmatrix}$

2.3. MASS MATRICES

The beam element is subjected to a distributed force of intensity F' in the z direction which can be obtained from equation (7). If $\{F'_b\}$ denotes the vector of four nodal forces equivalent to the distributed load F' acting on an element, then the work done by $\{F'_b\}$ and by F' during an arbitrary virtual displacement must be equal. If $\{\delta_b^*\}$ is the vector of virtual nodal displacements corresponding to the virtual displacement w^* within the element, then from equation (11)

$$w^* = [D]\{\delta_b^*\}. \quad (25)$$

Equating the work done by $\{F'_b\}$ and F' gives

$$\{\delta_b^*\}^T \{F'_b\} = \int_{v'} \{\delta_b^*\}^T [D]^T F' dv'. \quad (26)$$

Since this relation is true for any arbitrary virtual displacement, it can be written as

$$\{F'_b\} = \int_{v'} [D]^T F' dv'. \quad (27)$$

Obtaining F' from F in equation (7) and substituting into equation (27) yields

$$\{F'_b\} = \int_{v'} [D]^T (\rho \Omega^2 w \sin^2 \theta - \rho \ddot{w}) dv'. \quad (28)$$

Substituting for w from equation (11) into equation (28) gives

$$\{F'_b\} = \int_{v'} \{[D]^T \rho \Omega^2 \sin^2 \theta [D] \{\delta'_b\} - [D]^T \rho [D] \{\ddot{\delta}'_b\}\} dv'. \quad (29)$$

For harmonic vibrations and for constant cross sectional area

$$F'_b = (\Omega^2 \sin^2 \theta + \omega^2) [M'_b] \{\delta'_b\}, \quad (30)$$

where

$$[M'_b] = A\rho \int_0^l [D]^T [D] dx'. \quad (31)$$

The mass matrix $[M'_b]$ is given in Table 2.

TABLE 2

Mass matrices

$$[M'_b] = A\rho l \begin{bmatrix} 13 & & & \\ 35 & \text{Symmetric} & & \\ 11 & 1 & & \\ 210 & 105 & & \\ 9 & 13 & 13 & +\frac{m_t}{A\rho l} \\ 70 & 420 & 35 & \\ \frac{13}{420} & -\frac{1}{140} & -\frac{11}{210} & \frac{1}{105} \end{bmatrix}$$

Note: the term $m_t/A\rho l$ is present only for the last element of the beam; for other elements, $m_t = 0$.

2.3.1. Effect of tip mass

Addition of a tip mass increases the forces F_z and F_{in} by the amounts

$$F_{zt} = m_t \Omega^2 \sin^2 \theta w_t, \quad F_{int} = m_t \ddot{w}_t, \quad (32, 33)$$

where w_t represents the displacement at the tip of the beam. Since only the last element is associated with the tip of the beam the tip mass has an effect only on the mass matrix of the last element. The mass matrix $[M_{bt}]$ for the last element is also shown in Table 2.

2.4. DETERMINATION OF NATURAL FREQUENCIES AND MODE SHAPES

The stiffness matrices $[K'_{bt}]$ and the mass matrices $[M'_b]$ for all the elements are grouped together according to the sequence of the node numbering on the beam. The

rows and the columns corresponding to the nodes on the fixed edge are deleted to obtain the complete stiffness matrix $[K]$ and the complete mass matrix $[M]$ for the rotating cantilever beam with the tip mass. The equation of motion for the beam is

$$[K]\{\delta\} = \Omega^2 \sin^2 \theta [M]\{\delta\} - [M]\{\ddot{\delta}\}. \quad (34)$$

For the case of harmonic vibration with frequency ω , equation (34) can be expressed as

$$([K] - (\omega^2 + \Omega^2 \sin^2 \theta)[M])\{\delta\} = \{0\}, \quad (35)$$

whose solution will give the eigenvalues ($\omega^2 + \Omega^2 \sin^2 \theta$) and the mode shapes.

3. RESULTS

3.1. CONVERGENCE

The finite element results converge rapidly as shown in Table 3. Some of the results are compared with available results obtained by Kumar [5] and by Wang *et al.* [8] in Figures 4 through 8 for $\gamma = 0$. These results agree at low rotational speeds but deviate at high

TABLE 3
Convergence of the finite element model

Mode	Vibration frequency parameter α ($\gamma = 0, \Omega = 500$ rad/s, $R = 0$)		
	10 elements	12 elements	14 elements
First	12.7055	12.6001	12.5184
Second	38.5647	38.0503	37.6640
Third	80.2093	79.5985	79.1526
Fourth	140.621	139.965	139.504
Fifth	220.557	219.728	219.196
Sixth	320.678	319.336	318.572

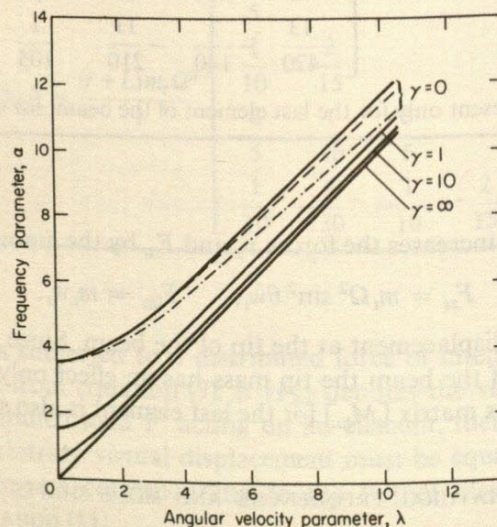


Figure 4. Variation of the first natural frequencies of vibrations with angular velocity for different values of γ . $R = 0$. —, Finite element; ——, Wang *et al.* [8]; - - -, Kumar [5].

Figure 5. Variation of the first natural frequency of vibrations with angular velocity for different values of γ . $R = 0$.

Figure 6. Variation of the first natural frequency of vibrations with angular velocity for different values of γ . Finite element.

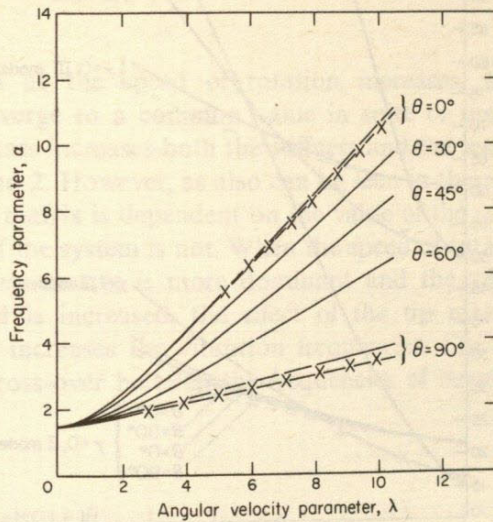


Figure 5. Variation of the first natural frequencies of vibrations with angular velocity for different values of θ . $\gamma = 1$; $R = 0$. —, Finite element; —x—, Kumar [5].

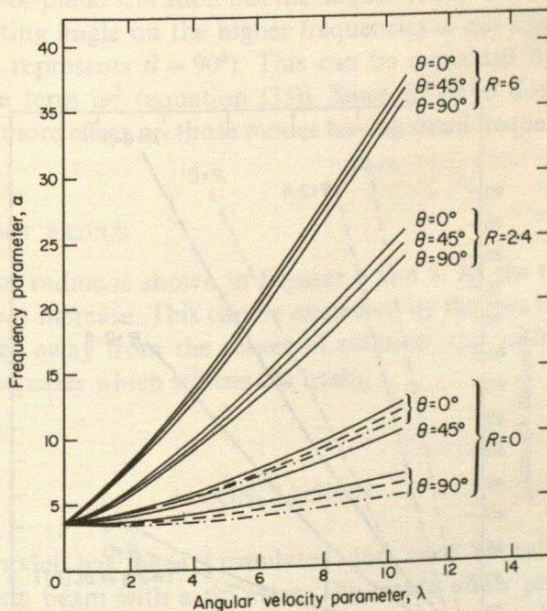


Figure 6. Variation of the first natural frequencies with angular velocity for different values of R , θ ; $\gamma = 0$. —, Finite element; —x—, Wang et al. [8]; -·-, Kumar [5].

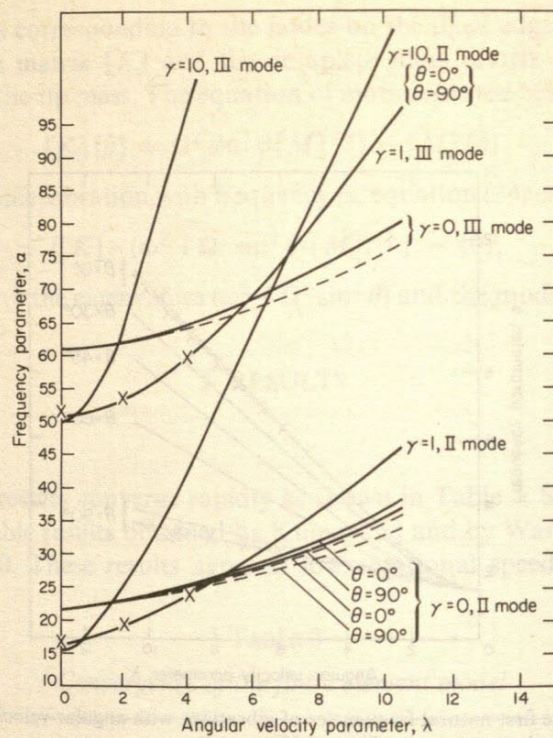


Figure 7. Variation of second and third natural frequencies with angular velocity for different values of γ .
 $R = 0, \theta = 0$. —, Finite element; ---, Wang *et al.* [8]; \times , Kumar [5].

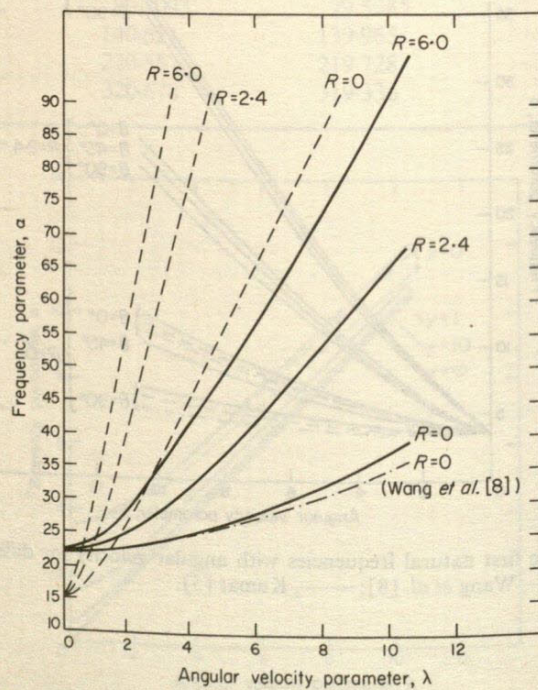


Figure 8. Variation of the second frequencies with angular velocity parameter for different values of R .
 $\gamma = 0$; ---, $\gamma = 10$.

rotational speeds. At high rotational speeds, the finite element method yields higher results while the Mykelstad method [5] yields lower results, respectively, than the extended Galerkin method [8].

3.2. EFFECT OF TIP MASS

Figure 4 shows that as the speed of rotation increases, the first mode natural frequencies tend to converge to a common value in spite of the difference in tip mass values. Adding the tip mass increases both the stiffness and the mass of the system, as can be seen from Tables 1 and 2. However, as also can be seen in these tables, the effect of the tip mass on the stiffness matrix is dependent on the value of the rotational speed whereas its effect on the inertia of the system is not. When the speed of rotation is low, the effect of the tip mass on the mass matrix is more dominant and the vibration frequencies are decreased. As the speed is increased, the effect of the tip mass on the stiffness also increases which in turn increases the vibration frequencies. For higher mode vibration frequencies, there is a cross-over between the frequencies of beams carrying different tip masses.

3.3. EFFECT OF SETTING ANGLE θ

The effect of the setting angle on the first mode frequencies is shown in Figures 5 and 6. When $\theta = 0^\circ$, the vibration is out of the plane of rotation and when $\theta = 90^\circ$, the vibration is in the plane of rotation. The vibration frequencies are affected by the term $\Omega^2 \sin^2 \theta$ indicating that the out-of-plane vibration has the largest frequencies.

The effect of the setting angle on the higher frequencies is not significant (see Figure 7 where the dotted line represents $\theta = 90^\circ$). This can be explained by comparison of the term $\Omega^2 \sin^2 \theta$ and the term ω^2 (equation (35)). Since $\Omega^2 \sin^2 \theta$ does not vary with the different modes, it has more effect on those modes having small frequencies (ω^2).

3.4. EFFECT OF THE ROOT RADIUS

The effect of the root radius is shown in Figures 6 and 8. As the root radius increases, the vibration frequencies increase. This can be explained by the fact that as the root of the beam is located further away from the center of rotation, the centrifugal force on each element of the beam increases which stiffens the beam.

4. CONCLUSION

A finite element model has been formulated and used to calculate the vibration frequencies of a rotating beam with a tip mass. The results show partial agreement with results obtained by previous investigators. These results show that the tip mass depresses the vibration frequencies at low speeds of rotation but it increases the vibration frequencies at high speeds of rotation. The setting angle θ has more effect on the first mode frequencies than on the higher mode frequencies. Also, the larger the root radius, the larger the vibration frequencies. The potential advantage of this method is that its principle can be applied to the investigation of the vibration frequencies of a rotating blade with a weighted edge.

ACKNOWLEDGMENT

Financial assistance from the National Science and Engineering Research Council of Canada through grant No. A0413 and from the Ford Motor Company of Canada Limited, are greatly appreciated.

REFERENCES

1. S. V. HOA 1978 *Journal of Sound and Vibration* **61**, 427–436. Vibration frequency of a curved beam with tip mass.
2. G. H. HANDELMAN, W. E. BOYCE and H. COHEN 1958 *Proceedings of the Third U.S. National Congress of Applied Mechanics*, Providence, Rhode Island, 175–180. Vibrations of a uniform rotating beam with tip mass.
3. W. E. BOYCE and G. H. HANDELMAN 1961 *Zeitschrift für angewandte Mathematik und Physik* **12**, 369–392. Vibrations of rotating beam with tip mass.
4. L. H. JONES 1975 *Quarterly of Applied Mathematics* **33**, 193. The transverse vibration of a rotating beam with tip mass; the method of integral equations.
5. R. KUMAR 1974 *Transactions of the C.A.S.I.* **7**, 1–5. Vibrations of space booms under centrifugal force field.
6. S. PUTTER and H. MANOR 1978 *Journal of Sound and Vibration* **56**, 175–185. Natural frequencies of radial rotating beams.
7. M. A. DOKAINISH and S. RAWTANI 1971 *International Journal of Numerical Methods in Engineering* **3**, 233–248. Vibration analysis of rotating cantilever plates.
8. J. T. S. WANG, O. MAHRENHOLTZ and J. BÖHM 1976 *Solid Mechanics Archives* **1**, 341–365. Extended Galerkin's method for rotating beam vibrations using Legendre polynomials.
9. K. K. KAPOOR and B. J. HARTZ 1966 *Journal of the Engineering Mechanics Division, Proceedings of the American Society of Civil Engineers* **EM2**, 177–195. Stability of plates using the finite element method.

APPENDIX: NOMENCLATURE

A	cross section of element	L	length of beam
c	$rl(m-n)+(l/2)(m^2-n^2)$	m	total number of elements
c^*	$R'(m-n)+\frac{1}{2}(m^2-n^2)$	m_t	tip mass
c_1-c_4	unknown coefficients	$[M]$	beam mass matrix
d	$R'+n$	$[M_b]$	element mass matrix
$[D]$	matrix given by equation (11a)	$[M_{bt}]$	mass matrix of element with tip mass
E	Young's modulus	n	number of elements before and not including the element under consideration (Figure 3)
F_r	radial centrifugal force	r	radius of disc
$F_{x,y}$	X, Y component of centrifugal force respectively	R	r/L
$F_{x,y,z}$	x, y, z component of centrifugal force respectively	R'	r/l
F_x'	local force in x' direction	V	potential energy (general expression)
F_{in}	inertia force	V_1	potential energy for non-rotating element without tip mass
F'	distributed force acting on element	V_2	potential energy due to centrifugal stiffening
$\{F_b\}$	nodal forces acting on element	V_{tip}	potential energy due to tip mass
h	thickness of beam	v'	volume of element
I	moment of inertia	w	lateral displacement in the z direction
$[K]$	stiffness matrix of beam	w^*	virtual displacement
$[K_{b1}]$	stiffness matrix (non-rotating beam without tip mass)	\ddot{w}	second derivative of displacement with respect to time
$[K_{b2}]$	centrifugal stiffness matrix	$w_{a,b}$	nodal displacements at a, b respectively
$[K_{bt}]$	tip mass stiffness matrix		
$/$	stiffness matrix for element length of element		

$w_{x'a,b}$	nodal slopes at a, b respectively	$\{\delta_b^*\}$	virtual displacements
x, y, z	global co-ordinate axes with origin at the root of the beam (Figure 1)	ε	non-dimensional variable
X, Y, Z	global co-ordinate axes with origin at the center of disc (Figure 1)	λ	$\Omega(\rho AL^4/EI)^{1/2}$, angular velocity parameter
x', y', z'	local co-ordinate for element	Ω	angular velocity (rad/s)
α	$\omega(\rho AL^4/EI)^{1/2}$, vibration frequency parameter	θ	setting angle
$\{\delta\}$	beam nodal displacements	ω	vibration frequency (rad/s)
$\{\delta_b\}$	element nodal displacements (equation (11a))	γ	$m_t/\rho AL$, tip mass parameters
		ρ	mass density
		σ_x	axial stress in element
		$\tau_{x'y'}$	shear stress in element

Department of Mechanical Engineering
Technion Institute of Technology, Haifa, Israel

Received 17 January 1978; revised 12 March 1978

The moment equations associated with the motion of the beam due to non-stationary random excitation by both deterministic envelope function and Gaussian noise are derived by an iterative single integration procedure. Numerically by digital computer, numerical results are obtained for two-degree-of-freedom systems which are excited by random excitation having envelope function. The results are given for the mean-square response versus the parameter ε . The effect of the numerical integrator results on the response does not exhibit significant sensitivity to the system of almost connected with the Gaussian noise.

1. INTRODUCTION

The non-stationary random response of a mechanical system to a non-stationary random excitation is one of major interest in the theory of random vibration. The non-stationary random excitation can be represented by a time-varying envelope function times the Gaussian noise. The mean-square response can be obtained by the spectral density approach or the spatial density approach. In the present paper, an approximate numerical method based on the finite-difference method is used to obtain the mean-square response. A recursive scheme involving trapezoidal rule can be applied to a continuous system by dividing the system into a discrete form of the spectrum. The recursive scheme has been used in previous researches and the results are numerically good for a small number of elements. In order to obtain more accurate results for higher values of the number of elements, the trapezoidal rule is used. The results of the present paper are compared with those of the previous work.

